Available online at www.sciencedirect.com

ScienceDirect

Current Opinion in Chemical Engineering

Review

Limits of Knallgas bacteria for autotrophic CO_2 conversion: physiology, H_2 kinetics and reactor constraints

Vivien Jesenofsky, Johannes Gescher and Miriam Edel

Aerobic hydrogen-oxidizing bacteria, commonly referred to as Knallgas bacteria, are chemoautotrophic microorganisms that oxidize molecular hydrogen (H_2) while fixing carbon dioxide (CO_2) into cellular material. Historically studied as model systems for lithoautotrophic metabolism, these organisms have regained attention due to their potential for renewable H_2 utilization, land-independent biomass production, and electrochemically coupled CO_2 conversion. Among them, *Cupriavidus necator* has emerged as a promising industrial platform, while thermophilic and high-affinity H_2-oxidizers such as *Kyrpidia spormannii* are increasingly explored in bioelectrochemical systems. Despite growing interest, substantial gaps remain between laboratory demonstrations and scalable industrial performance. This review analyzes the physiological characteristics of Knallgas bacteria, including growth kinetics and H_2 oxidation parameters, and evaluates their translation into gas fermentation and oxic microbial electrosynthesis systems. Particular emphasis is placed on key engineering limitations, including H_2 mass transfer, electron partitioning during aerobic metabolism, reactor safety constraints, and electrochemical surface scaling.

Address
Institute of Technical Microbiology, University of Technology Hamburg, Hamburg, Germany

Corresponding author: Edel, Miriam (miriam.edel@tuhh.de)

Current Opinion in Chemical Engineering 2026, **54**:101302

This review comes from a themed issue on **CO_2 bioconversion into valuable products**

Edited by **Sebastia Puig** and **Deepak Pant**

Available online xxxx

https://doi.org/10.1016/j.coche.2026.101302

2211–3398/© 2026 The Authors. Published by Elsevier Ltd. This is an open access article under the CC BY license (http://creativecommons.org/licenses/by/4.0/).

Introduction

Knallgas bacteria represent a phylogenetically diverse group spanning multiple bacterial phyla, including Proteobacteria (*Cupriavidus*, *Paracoccus*), Aquificae (*Hydrogenobacter*), and Firmicutes (*Kyrpidia*), that share the ability to oxidize molecular H_2 and fix CO_2 into biomass or other products using oxygen (O_2) as the terminal electron acceptor of their respiratory chain. In these organisms, H_2 oxidation is coupled to O_2 reduction, generating energy for autotrophic growth typically via the Calvin–Benson–Bassham (CBB) cycle. Knallgas bacteria were intensively studied for chemolithoautotrophic metabolism and hydrogenase biochemistry [1]. The global transition toward renewable energy systems and circular carbon utilization, driven by carbon pricing policies exceeding $100/ton CO_2 in leading markets and the projected $2.5 trillion H_2 economy by 2050, has fundamentally broadened the motivation to study these organisms.

Renewable H_2 supports indirect electrification of microbial production systems. In gas fermentation processes, H_2-oxidizing bacteria utilize H_2 and O_2 to enable autotrophic CO_2 fixation, thereby decoupling microbial production from reduced organic substrates. Among these organisms, *C. necator* has emerged as the most developed production platform due to its relatively high autotrophic growth rates, metabolic versatility, and genetic accessibility [2,3]. High cell densities have been achieved in pressurized gas-fed reactors employing *C. necator* [3], and H_2-oxidizing strains such as *Paracoccus versutus* have been investigated for single-cell protein production under autotrophic conditions [4]. Decoupling biomass production from agricultural land is relevant to growing protein demand and limited arable resources. Integrating *in situ* electrochemical H_2 generation with microbial CO_2 fixation enables reactor concepts that may improve upon conventional water electrolysis. In oxic microbial electrosynthesis (oMES), H_2 is generated in situ at cathodes and directly consumed by aerobic H_2-oxidizers [5]. Hence, the problem of explosive mixtures can be circumvented by the direct microbial depletion of H_2 at the cathode surface. Moreover, the applied voltage can be reduced by 0.3–0.8 V compared to conventional electrolysis due to biocatalytic H_2 consumption, potentially improving overall system efficiency. This concept could pave the way for even more efficient biomass production as a novel protein resource, as shown by Pous and colleagues in a study using a mixed culture enriched in H_2-oxidizing bacteria [6].

Knallgas bacteria are frequently discussed alongside acetogenic microorganisms in the context of H_2-based CO_2 conversion. While both groups utilize H_2 as an electron donor, their metabolic strategies differ essentially. Acetogens operate under strictly anoxic conditions and channel electrons directly into reduced products via the Wood–Ljungdahl pathway, whereas Knallgas bacteria rely on aerobic respiration and partition electrons between energy generation and biosynthesis. The use of the Wood–Ljungdahl pathway allows the very electron-efficient production of a limited spectrum of end-products. The low amount of available energy from acetogenesis, on the other hand, is the reason why genetic engineering towards more complex end-products is extremely difficult, and biomass accumulation rates are typically low compared to Knallgas bacteria. Despite promising applications, technical and economic hurdles limit industrial implementation. Bringing the potential of Knallgas bacteria to an application requires a systematic understanding of the hierarchical constraints that limit performance. The following sections combine intrinsic physiological parameters, including growth kinetics and H_2 oxidation rates, with reactor-level constraints such as gas transfer, electron partitioning, electrochemical current density, and operational safety. By systematically distinguishing biological potential from physical and thermodynamic boundaries, the realistic engineering limits of Knallgas-based CO_2 conversion can be defined, and the most promising intervention points identified.

Functional landscape of Knallgas bacteria

Autotrophic growth capacity

Under defined autotrophic conditions, Knallgas bacteria exhibit substantial diversity in growth kinetics. As summarized in Table 1, there is no apparent difference regarding growth rate when comparing different CO_2 fixation pathways. However, comparison of biomass yields per mole of H_2 consumed suggests that the thermodynamically more efficient reductive tricarboxylic acid (rTCA) cycle may support higher biomass yields than the CBB cycle.

The organisms compiled in Table 1 illustrate the broad physiological range of H_2-oxidizing bacteria, spanning thermophilic rTCA specialists, mesophilic sulfur oxidizers, and classical Knallgas bacteria such as *C. necator*. In contrast, purple nonsulfur bacteria, which can also grow under dark chemolithoautotrophic conditions, exhibit substantially lower intrinsic growth rates, displaying doubling times of 22 to 27 hours, potentially reflecting the energetic constraints of this metabolic niche [14].

H_2 oxidation kinetics as the rate-determining interface

Beyond carbon fixation, H_2 oxidation kinetics strongly influence the ecological and biotechnological performance of Knallgas bacteria. The representative organisms summarized in Table 2 illustrate the wide range in H_2 affinity and uptake capacity among aerobic H_2-oxidizing bacteria. *Kyrpidia spormannii* exhibits a high-affinity phenotype with a submicromolar K_s (327 ± 24 nM), whereas *Paracoccus denitrificans*, *C. necator*, and *Hydrogenovibrio marinus* operate in the micromolar range [8,11,15–21]. Reported maximum H_2 uptake capacities also span several orders of magnitude. However, these differences reflect both biological diversity and substantial variation in experimental methodology.

H_2 affinity (K_s or K_m) and maximum H_2 uptake capacities (V_{max} or equivalent activity measures) are reported as originally published. Experimental conditions, assay type, and normalization methods are summarized in Supplementary Table S2 to improve transparency. These parameters were not standardized because the underlying kinetic assays differ substantially among studies (e.g. whole-cell versus manometric assays, different normalization bases, assay conditions, and reporting formats), preventing direct quantitative comparison.

Nevertheless, the parameters compiled in Table 2 demonstrate that H_2 affinity alone does not determine physiological performance. Rather, high-affinity organisms may be advantageous under diffusion-limited conditions, whereas organisms with higher uptake capacities

Table 1

Intrinsic autotrophic growth rates and H_2 biomass yields of representative H_2-oxidizing bacteria.

Organism	Mode / Setup	μ (h^{-1})	$Y_{X/H2}$ (g DW mol^{-1} H_2)	Pathway	Source
Hydrogenobacter thermophilus	Gas fermentation (70°C)	0.42	n/a	rTCA	[7]
Hydrogenovibrio marinus	Gas fermentation (37°C)	0.088	5.5	CBB	[8]
Thiomicrolovo sp.	Gas fermentation (28°C)	0.46	6.07	rTCA	[9]
C. necator	Gas fermentation (30°C)	0.42	4.6	CBB	[10]
K. spormannii	Gas fermentation (55°C)	0.19	4.3	CBB	[11]
C. necator	oMES (Planktonic, 30°C)	0.09	n/a	CBB	[12]
K. spormannii	oMES (Cathodic Biofilm, 60°C)	0.046	n/a	CBB	[13]
Rhodococcus opacus	Dark chemoautotrophy (30°C)	0.044	n/a	CBB	[8]

Original values, experimental conditions, and calculation details are provided in Supplementary Table S1.

Table 2

H_2 oxidation kinetics of representative Knallgas bacteria.

Organism	Kinetic Regime	H_2 Affinity (K_s or K_m)	Max. H_2 Uptake Capacity (V_{max})	Source
Kyrpidia spormannii (FAVT5)	High-affinity	K_s = 327 ± 24 nM	60 ± 3 $nmol\,min^{-1}\,mg^{-1}_{DW}$	[11]
Cupriavidus necator (H16)	Intermediate/High-flux	K_m = 4.6 μM*(whole cell)*	440–1530 $nmol\,min^{-1}\,mg^{-1}_{DW}$*(growth-derived max H_2 flux,μ = 0.12–0.42h^{-1})*	[15,16]
Paracoccus denitrificans	Micromolar	K_m=1 μM	V_{max} = 3.63 fmol·h^{-1}·$cell^{-1}$	[17]
Hydrogenovibrio marinus MH-110 / DSM 11271	High-flux	K_m = 12 μM*(purified membrane-bound hydrogenase)*	185 $U{\cdot}mg^{-1}_{protein}$*(purified enzyme, 30°C)*;465 nmol·min^{-1}·mg_{DW}-1*(growth-derived max H_2 flux)*	[8,19]
Hydrogenomonas facilis	High-activity *(manometric)*	n/a	536 $nmol\,min^{-1}\,mg^{-1}_{DW}$*(whole cell, O_2-driven, autotrophic, Warburg manometry)*	[21]

Reported H2 affinities (Ks or Km) and maximum H_2 uptake capacities (Vmax or equivalent activity measures) of representative H_2-oxidizing bacteria. Original values, experimental conditions, assay characteristics, and normalization methods are provided in the Supplementary Table S2.

may perform better when H_2 is continuously supplied. Accordingly, selecting a strain whose kinetic characteristics match the intended reactor architecture while balancing H_2 affinity and total uptake capacity is a prerequisite for achieving high productivity.

Energetic constraints of aerobic H_2 oxidation

Even under conditions where H_2 supply is not limiting, additional energetic constraints arise from the architecture of aerobic H_2 metabolism. Most Knallgas bacteria summarized in Table 1 fix CO_2 via the CBB cycle, while electrons derived from H_2 oxidation are simultaneously used for ATP generation through oxygen respiration. Reiner et al. note that approximately half of the electrons consumed by aerobic autotrophs are expended in respiratory energy generation rather than incorporated into biomass or product [5]. This partitioning reduces theoretical carbon fixation yields relative to strictly reductive anaerobic pathways such as the Wood–Ljungdahl pathway in acetogens. Strategies to circumvent these constraints range from regulatory optimization to complete pathway replacement. Modest improvements have been achieved through overexpression of CBB cycle transcriptional regulators (cbbR and regA), yielding 11% increased biomass accumulation [22]. More ambitious approaches have targeted the complete replacement of the inefficient CBB cycle with synthetic alternatives. The most successful implementation to date is the reductive glycine pathway in *C. necator*. This synthetic route bypasses RuBisCO entirely, utilizing formate, which can be generated electrochemically from H_2 and CO_2 as a carbon feedstock. Initial implementation by Claassens et al. demonstrated proof-of-concept formatotrophic growth, achieving 2.6 g CDW mol^{-1} formate compared to 2.9 g CDW mol^{-1} for the wild-type CBB cycle strain [23]. Through systematic optimization and complete genome integration, Dronsella et al. achieved a breakthrough 17% biomass yield improvement (4.52 vs 3.86 g CDW mol^{-1} formate) in chemostat cultures, representing the first demonstration that synthetic pathways can exceed natural carbon fixation efficiency [24]. However, this approach involves significant trade-offs, including a longer doubling time and the requirement for formate as feedstock rather than direct H_2 utilization.

Standardized comparison of realized autotrophic productivities

While microbial physiology defines intrinsic growth potential (Table 1) and H_2 uptake capacity (Table 2), realized productivity is primarily determined by reactor engineering. To enable comparison across studies, reported autotrophic production rates were standardized to volumetric productivity (g L^{-1} d^{-1}) and carbon productivity (g C L^{-1} d^{-1}). The resulting dataset, summarized in Table 3, compares representative Knallgas

production systems across gas fermentation, packed-bed, and electrochemical reactor configurations.

The standardized comparison presented in Table 3 focuses on realized volumetric and carbon productivity as common engineering performance metrics. While these metrics facilitate comparison across diverse autotrophic production systems, the reported values are also influenced by reactor-specific operating conditions, including gas flow rate, gas residence time, pressure, gas composition, mixing, and reactor configuration, which vary considerably between studies and therefore cannot be standardized quantitatively. Similarly, a systematic comparison of product-specific quality attributes is not feasible because these parameters are highly product-dependent and are assessed using different analytical methods and reporting criteria across the literature. Therefore, the productivity metrics presented here should be interpreted within the context of both the applied process conditions and the respective product quality.

Across the studies summarized in Table 3, the highest productivity remains the pressurized stirred-tank gas fermentation reported by Ishizaki and Tanaka, which achieved 36 g L^{-1} PHB within 60 h (14.4 g L^{-1} d^{-1}) [10]. This early study established the productivity benchmark for autotrophic PHB synthesis from H_2 and CO_2 and demonstrated the performance achievable under conditions of intense gas–liquid mass transfer. Later pressurized systems reached comparable performance. For example, Volova et al. reported 10.8 g L^{-1} d^{-1} PHB in a pressurized stirred-tank reactor operating at $k_{La} \approx 460h^{-1}$, achieved through high agitation and gas recirculation [28]. However, achieving such high gas-transfer rates requires substantial energy input, as discussed in section H_2 transfer and operational boundaries. Thus, in stirred-tank Knallgas fermentations, H_2 mass transfer defines the upper bound of achievable carbon fixation rates, with biological capacity frequently underutilized because H_2 delivery cannot match enzymatic turnover capacity. In contrast, atmospheric laboratory reactors typically achieve substantially lower productivities. The stirred-bottle gas reactor described by Lambauer and Kratzer produced 10.2 g L^{-1} PHB within 150 h (1.63 g L^{-1} d^{-1}), while packed-bed gas reactors achieve lower but still substantial PHB productivities of approximately 1.44 g L^{-1} d^{-1} through improved gas–solid contact but reduced bulk mixing [30,35]. Electroautotrophic systems, summarized in Table 3, exhibit even lower volumetric productivities. In microbial electrosynthesis reactors, PHB formation rates generally remain below 0.1 g L^{-1} d^{-1}, reflecting limitations in H_2 evolution rate and interfacial mass transfer [31,32]. Overall, these studies demonstrate that the highest realized productivities are consistently achieved in reactor configurations providing the greatest H_2 transfer capacity. Although specific growth rates may approach $0.2h^{-1}$ under optimized physiological conditions, the production rates summarized in Table 3 correlate strongly with reactor-level H_2 delivery.

Reactor-level constraints and engineering architectures

Despite their high intrinsic metabolic capacity, Knallgas systems are primarily constrained by reactor-level H_2 delivery. Industrial biotechnology relies predominantly on stirred-tank reactors, where gas transfer depends on mixing and sparging [44]. Consequently, gas fermentation systems are engineered to maximize interfacial transfer through agitation, pressurization, or gas recirculation, often increasing energy demand and operational complexity [45].

H_2 transfer and operational boundaries

In conventional stirred-tank gas fermentations, H_2 must be transferred from the gas phase into the aqueous phase before cellular oxidation can occur. However, H_2 exhibits low aqueous solubility (~0.8 mM at 1 bar and 25°C) and a volumetric mass transfer coefficient (k_{La}) approximately 30%–40% lower than O_2 under comparable agitation conditions [46,47]. This creates a fundamental kinetic mismatch: dissolved H_2 concentrations frequently range from 0.5 to 2.0 μM in typical reactor operations, which can overlap with or fall below the H_2 affinity constants reported for Knallgas bacteria (Table 2). Thus, H_2 availability can limit cellular H_2 oxidation under typical reactor conditions. Pressurization provides proportional improvements in H_2 availability: an H_2 partial pressure of 5 bar increases dissolved H_2 to ~4 mM, but also increases safety complexity. Industrial benchmark systems illustrate this relationship: Volova et al. achieved 10.8 g L^{-1} d^{-1} PHB productivity at k_{La} = $460h^{-1}$ with high agitation rates, while Lu and Yu reported more modest but sustainable productivities (1.44 g L^{-1} d^{-1}) at k_{La} values of $357h^{-1}$ for O_2 in packed-bed configurations [28,30]. The energetic cost of achieving high k_{La} values becomes prohibitive: increasing agitation from 200 to 800 rpm typically raises power consumption by 8–16-fold while providing only 2–3-fold improvements in H_2 transfer [1]. Consequently, further increases in productivity require improvements in H_2 delivery rather than microbial physiology alone, making reactor design the principal determinant of process performance.

The severity of this transport limitation is configuration-dependent. In stirred-tank reactors, the achievable H_2 transfer rate is set by the product of k_{La} and the gas–liquid driving force (the difference between the saturation and bulk dissolved-H_2 concentrations). The k_{La} is raised primarily through mechanical agitation, at steeply rising power cost, while pressurization increases the driving force by raising the dissolved-H_2 saturation

Table 3

Standardized autotrophic production performance under Knallgas conditions. *

Organism	Product	Reactor	Time (h)	$Titer_{max}$ (g/L)	Volumetric rate ($g \cdot L^{-1} \cdot d^{-1}$)	Carbon productivity ($g\ C \cdot L^{-1} \cdot d^{-1}$)	Source
C. necator ATCC 17697	PHB	Pressurized gas fermentation (STR)	60	36	14.4	8.04	[10]
C. necator ATCC 17697	PHB	Airlift gas fermentation	120	49	9.84	5.49	[25]
C. necator	PHB	Gas fermentation (STR)	76	12	3.8	2.12	[26]
*C. necator*B-5786	PHB	Gas fermentation (STR)	72	12	4	2.23	[27]
C. eutrophus B-10646	PHB	Gas fermentation (STR)	80	36	10.8	6.03	[28]
C. necator DSM 545	PHB	Two-stage gas fermentation* (STR)	100	11	2.78	1.55	[29]
C. necator	PHB	Packed-bed gas reactor	56	3.35	1.44	0.8	[30]
Engineered *C. necator*	PHB	Microbial electrosynthesis (MES)*	120	0.485	0.097	0.05	[31]
C. necator H16	PHB	Gas fermentation (Batch)	144	0.27	0.05	0.03	[32]
C. necator H16	PHB	Gas fermentation (Batch)	72	14.2	4.7	2.64	[33]
Recombinant *C. necator*	P(3HB-co-3HHx)	Gas fermentation (STR)	120	7.8	1.56	0.87	[34]
C. necator	PHB	Gas fermentation (stirred-bottle reactor)	150	10.2	1.63	0.91	[35]
C. necator LH74D	Isobutanol & 3-methyl-1-butanol	MES (formate-driven)*	100	n/a	0.034	0.022	[36]
Engineered *C. necator*	2-hydroxyisobutyric acid	Gas fermentation (STR)	504	3.2	0.15	0.07	[37]
C. necator Re2061	C15–C17 alkenes	Two-stage gas fermentation* (STR)	56	0.0044	0.0019	0.0016	[38]
*C. necator*pKR-hum	α-humulene	Gas fermentation (septum flask)	120-144	0.0063	0.0011	0.00097	[39]
C. necator H16	Acetoin	Continuous gas fermentation (STR)	336	3.9	0.28	0.15	[40]
C. necator H16	2,3-butanediol	Gas fermentation (STR)	n/a	n/a	0.947	0.505	[41]
Paracoccus denitrificans Y5	SCP	Gas fermentation (Batch)	120	1.56	0.31	0.135	[4]
C. necator Re2133	Isopropanol	Pressurized gas fermentation (STR)	85	n/a	0.99	0.59	[42]
C. necator R3	SCP	Gas fermentation (STR)	120	13.8	2.76	1.46	[43]

Original reported values and the standardization procedure used to calculate volumetric and carbon productivities are summarized in Supplementary Tables S3 and S4, including the corresponding data sources within each original publication. Stirred tank reactor (STR): Pressurized reactors may include gas recirculation loops to improve gas utilization efficiency.

* Indicates related electrochemical or hybrid systems that are not strictly Knallgas fermentations.

concentration. Airlift and bubble-column reactors avoid mechanical agitation and therefore operate at lower and less tunable k_{La}, but at reduced shear and energy demand, which can favor long-term biological stability [25]. Packed-bed configurations shift the controlling resistance from bulk gas–liquid transfer to gas–solid and liquid–film transfer at the biocatalyst surface, improving local H_2 availability and gas utilization while sacrificing bulk mixing [30]. Membrane- and electrode-based systems (section Reactor systems as H_2 delivery platforms) remove the bulk gas–liquid step altogether by delivering H_2 directly at a solid interface [48,49]. The same intrinsic kinetic limitation therefore manifests as a power-limited k_{La} ceiling in sparged reactors, as a diffusion-limited film resistance in packed beds, and as an interfacial flux limit in membrane and electrochemical systems.

Safety envelope and O_2 co-feeding

The simultaneous requirement for H_2 and O_2 creates fundamental safety constraints governed by well-defined flammability limits. H_2-air mixtures are explosive between 4.0 and 75.0 vol% H_2, with the lower explosion limit decreasing to 4.0 vol% in pure O_2. At 10 bar, the explosive range widens to 3.0–80.0 vol% [50,51]. Early physiological studies quantified O_2 sensitivity of hydrogenase activity, with *Hydrogenomonas facilis* showing reversible inhibition above 5% O_2 in the gas phase, corresponding to dissolved O_2 concentrations > 0.2 mM [21]. Modern reactor systems must balance respiratory O_2 demand, typically requiring dissolved O_2 concentrations of 0.1–0.4 mM for aerobic growth, against hydrogenase sensitivity and explosion risk [47].

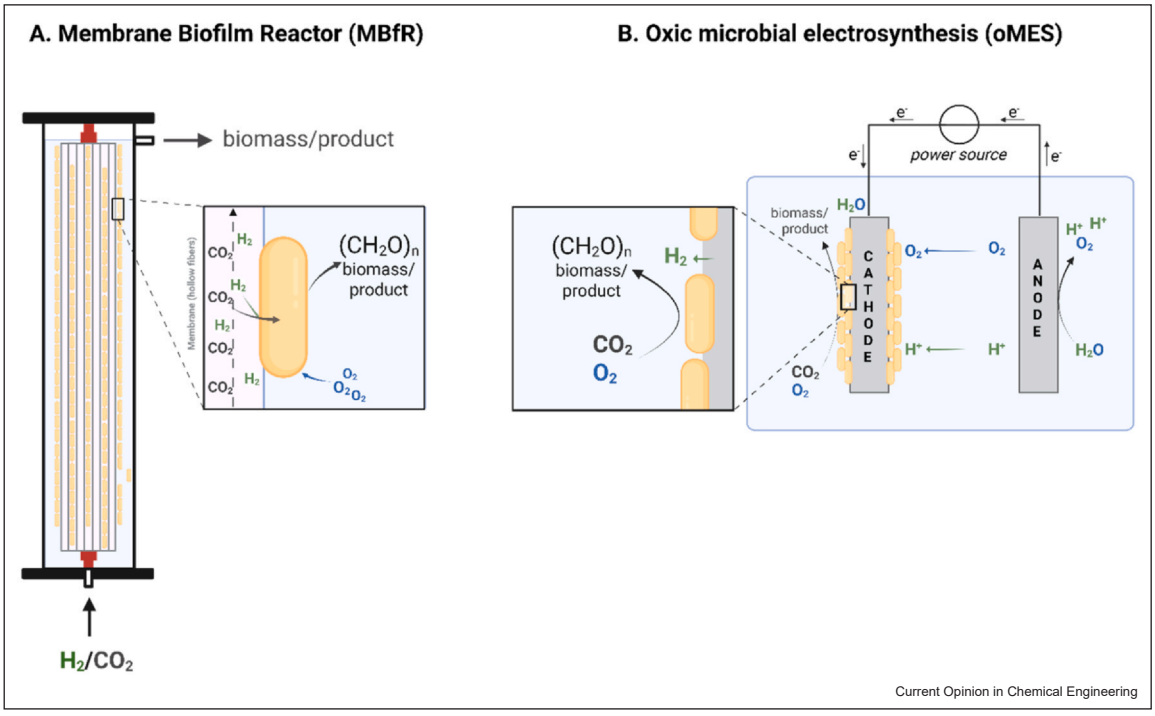
The flammability limits given above refer to H_2 in air, that is, against a fixed high-O_2 background. In an operating bioreactor, however, the O_2 fraction is itself a controlled variable, and the relevant boundary is the limiting oxygen concentration (LOC), the O_2 level below which no H_2/O_2/inert mixture propagates a flame, essentially independent of H_2 content. For H_2, this LOC is as low as 4.6 vol% O_2 [52]. This asymmetry is decisive for reactor operation. Because H_2 must be kept high to sustain mass transfer (section H_2 transfer and operational boundaries), it cannot be lowered for safety without sacrificing productivity, whereas O_2 can be displaced with inert gas or CO_2. Holding the gas-phase O_2 fraction below its LOC is therefore the robust inerting strategy, rendering the atmosphere nonflammable even at the high H_2 partial pressures needed for efficient transfer. In sparged stirred-tank and airlift systems, H_2 and O_2 co-accumulate in a shared headspace whose composition must be actively held outside the flammable envelope — by limiting the O_2 feed below the LOC, diluting with inert carrier gas, and minimizing headspace volume and gas residence time to reduce the free-gas inventory. Continuous active sparging maximizes transfer but constantly regenerates a potentially explosive headspace, whereas passive diffusive or membrane-mediated supply keeps the free H_2 inventory small and confines H_2 largely to the liquid or biofilm phase. Membrane biofilm reactors and oMES systems address the hazard structurally rather than operationally, because membrane supply spatially separates the H_2 and O_2 streams (section Reactor systems as H_2 delivery platforms), and in oMES, H_2 is generated and consumed in situ at the cathode before a bulk gas phase can form. In these configurations, the safety problem is reframed from controlling a headspace composition into managing local interfacial H_2 and O_2 fluxes.

Reactor systems as H_2 delivery platforms

Given the transport and safety constraints associated with conventional gas sparging, alternative reactor architectures increasingly focus on surface-associated growth and controlled H_2 delivery rather than bulk gas–liquid transfer. Although industrial biotechnology has historically relied almost exclusively on stirred-tank reactors, biofilm-based systems offer several potential advantages, including high biomass densities, plug-flow operation, and improved catalyst stability [44]. One implementation of this concept is the membrane biofilm reactor (MBfR), which is specifically designed to optimize H_2 delivery in Knallgas systems (Figure 1a). In MBfRs, H_2 and CO_2 are supplied through gas-permeable hollow-fiber membranes, allowing H_2 to diffuse directly from the membrane lumen into an attached microbial biofilm. The membrane surface, therefore, acts as a controlled H_2 interface, allowing localized H_2 transfer to H_2-oxidizing bacteria while avoiding bulk gas bubbles and the safety constraints associated with mixed H_2/O_2 sparging. By eliminating the bulk gas–liquid transfer step and spatially separating H_2 supply from O_2 exposure, this configuration improves H_2 utilization efficiency and process control. Surface-to-volume ratios of 400–800 m^2/m^3 have been achieved in membrane biofilm reactors, providing substantial interfacial area for H_2 delivery while maintaining compact reactor footprints [53–55]. The membrane configuration fundamentally restructures the transport challenge rather than merely redistributing resistance. While biofilm thickness and membrane–biofilm diffusion still influence local H_2 availability, the elimination of bulk gas–liquid transfer and improved safety profile enable operation at higher H_2 partial pressures and enhanced utilization efficiencies. Long-term operation requires management of biofilm stability and membrane fouling, but these represent addressable engineering challenges rather than fundamental thermodynamic limitations.

Alternatively, electrochemical integration allows H_2 to be generated *in situ* at the cathode, enabling precise control of H_2 delivery while addressing safety constraints. As shown in Figure 1b, oMES couples water

Figure 1



(a) MBfR configuration in which H_2 is supplied through gas-permeable hollow fibers to an attached biofilm, while O_2 is delivered from the bulk liquid, enabling spatial separation of H_2 and O_2 supply. **(b)** Schematic of an oMES system where electrochemically generated H_2 mediates electron transfer from the cathode to H_2-oxidizing bacteria, enabling aerobic CO_2 fixation.

electrolysis directly to aerobic autotrophic metabolism. H_2 is generated *in situ* at the cathode via proton reduction, while O_2 is produced at the anode. H_2 diffuses across the electrode–biofilm interface and is oxidized by H_2-oxidizing bacteria, which simultaneously reduce O_2 and fix CO_2 into biomass or product. While H_2 mediates electron transfer into cellular metabolism, the electrochemical generation approach allows precise flux control while circumventing both bulk mass transfer bottlenecks and safety limitations that constrain traditional reactor designs. Studies with thermoacidophilic *K. spormannii* achieved CO_2-to-biomass Coulombic efficiencies reaching 28%, with nearly complete biotic electron utilization under optimized O_2 management that minimizes cathode side reactions [13]. Process energy analysis revealed solar energy requirements of 67.89 kWh kg^{-1} dry biomass for oMES systems, substantially outperforming traditional photosynthetic routes: C_3 plants (324.07 kWh kg^{-1}), C_4 plants (138.89 kWh kg^{-1}), and microalgae cultivation (111.11 kWh kg^{-1}). This efficiency advantage stems from superior photovoltaic energy conversion compared to biological photosynthesis in integrated electrochemical processes. The performance of electrochemical H_2 delivery depends on several design parameters, and many constraints encountered in conventional reactors persist in modified form. The cathode material is central as it should combine a low H_2 evolution overpotential with a high accessible surface area and good biocompatibility for cathodic biofilm colonization. Planar metal or graphite electrodes offer well-defined surfaces but limited volumetric area, whereas three-dimensional carbon materials: carbon felt, reticulated vitreous carbon, or highly porous structures such as aerographite, raise the electroactive surface-to-volume ratio and support higher volumetric H_2 evolution and current density, at the cost of more complex internal mass transport within the biofilm-colonized matrix [48,56]. Electrolyte composition governs ionic conductivity, buffering capacity, and local pH at the electrode. Reactor geometry — electrode spacing, the presence or absence of a membrane separating the electrode chambers, and flow-through versus batch operation — determines ohmic losses, O_2 cross-over between anode and cathode, and the supply of fresh medium and CO_2 to the biofilm [49,57]. Within this framework, the constraints discussed for gas-fed systems translate directly to electrochemical reactors as bulk H_2 mass transfer is replaced by interfacial H_2 flux and electron-transfer rate at the cathode. The O_2 safety envelope is managed intrinsically by microbial H_2 depletion but reappears as the need to suppress cathodic O_2 reduction as a competing side reaction [49,58]. The

volumetric-productivity ceiling set by k_{La} in sparged reactors is replaced by the available electroactive cathode surface area per reactor volume, making electrode architecture and surface-area scaling, rather than gas–liquid mass transfer, the primary engineering target for oMES [48]. Encouragingly, the feasibility of this surface-scaling route has already been demonstrated in a related, anoxic electrosynthesis context, where reactor architecture rather than intrinsic biology was shown to set the achievable productivity. Cabau-Peinado and colleagues demonstrated that microbial electrosynthesis can reach volumetric productivities comparable to established fermentation technologies [58]. Using an anoxic, directed flow-through electrochemical reactor with a porous biofilm-covered cathode, the authors enabled dense microbial colonization and increased volumetric current density, allowing continuous CO_2 reduction to C_2–C_6 carboxylic acids. This reactor configuration achieved productivities comparable to syngas fermentation and chain-elongation processes, challenging the common assumption that bioelectrochemical systems are inherently rate-limited [58].

Conclusion

Knallgas bacteria possess substantial capacity for autotrophic CO_2 fixation. Physiological studies demonstrate that intrinsic growth rates and H_2 oxidation kinetics are sufficient to sustain relatively rapid autotrophic metabolism [11,17]. However, the analysis presented in this review shows that the practical performance of Knallgas systems is governed primarily by engineering constraints rather than by biological capacity. Future progress in H_2-driven CO_2 conversion will therefore depend largely on improving H_2 delivery architectures and reactor-level transport efficiency. Reactor concepts that enhance interfacial H_2 flux, such as pressurized gas fermentation, membrane-based H_2 supply, or electrochemical H_2 generation, represent promising strategies for overcoming mass-transfer limitations [28,30,41,59]. Recognizing the coupled constraints of H_2 transfer, O_2 safety, and respiratory energetics provides a realistic framework for guiding future research and translating H_2-based autotrophic metabolism from laboratory demonstrations toward industrially relevant bioprocesses.

CRediT authorship contribution statement

Vivien Jesenofsky: Writing – original draft, Visualization. **Johannes Gescher:** Writing – review & editing, Conceptualization. **Miriam Edel:** Conceptualization, Project administration, Resources, Writing – review & editing.

Funding

This study was supported by the Deutsche Forschungsgemeinschaft (DFG, German Research Foundation) — SFB 1615 — 503850735 at the TUHH.

Data Availability

No data were used for the research described in the article.

Declaration of Competing Interest

The authors declare that they have no known competing financial interests or personal relationships that could have appeared to influence the work reported in this paper.

Acknowledgements

Graphical Abstract and Figure 1 were created in BioRender: Edel, M. (2026) https://BioRender.com/1eimenx and https://BioRender.com/klsm9ty.

Appendix A. Supporting information

Supplementary data associated with this article can be found in the online version at doi:10.1016/j.coche.2026.101302.

References and recommended reading

Papers of particular interest, published within the period of review, have been highlighted as:

- • of special interest
- •• of outstanding interest

1. Schlegel and Lafferty: **Novel Energy and Carbon Sources — A. The Production of Biomass from Hydrogen and Carbon Dioxide** (Chapter 6) by H. G. Schlegel and R. M. Lafferty; 1971.

2. Raberg M, Volodina E, Lin K, Steinbüchel A: ***Ralstonia eutropha* H16 in progress: applications beside PHAs and establishment as production platform by advanced genetic tools**. *Crit Rev Biotechnol* 2018, **38**:494-510, https://doi.org/10.1080/07388551.2017.1369933

3. Lin L, Huang H, Zhang X, Dong L, Chen Y: **Hydrogen-oxidizing bacteria and their applications in resource recovery and pollutant removal**. *Sci Total Environ* 2022, **835**:155559, https://doi.org/10.1016/j.scitotenv.2022.155559

4. Dou J, Huang Y, Ren H, Li Z, Cao Q, Liu X, Li D: **Autotrophic, heterotrophic, and mixotrophic nitrogen assimilation for single-cell protein production by two hydrogen-oxidizing bacterial strains**. *Appl Biochem Biotechnol* 2019, **187**:338-351, https://doi.org/10.1007/s12010-018-2824-1

5. • Reiner JE, Korth B, Edel M: **Oxygen in the mix: is oxic microbial electrosynthesis a potential alternative for biomass production?** *ChemElectroChem* 2024, https://doi.org/10.1002/celc.202400397.
This review discusses the emerging concept of oMES and its potential advantages for microbial biomass and product formation.

6. Pous N, Balaguer MD, Matassa S, Chiluiza-Ramos P, Bañeras L, Puig S: **Electro-cultivation of hydrogen-oxidizing bacteria to accumulate ammonium and carbon dioxide into protein-rich biomass**. *Bioresour Technol Rep* 2022, **18**:101010, https://doi.org/10.1016/j.biteb.2022.101010

7. Kawasumi T, Igarashi Y, Kodama T, Minoda Y: ***Hydrogenobacter thermophilus* gen. nov., sp. nov., an extremely thermophilic, aerobic, hydrogen-oxidizing bacterium**. *Int J Syst Bacteriol* 1984, **34**:5-10, https://doi.org/10.1099/00207713-34-1-5

8. Cantera S, Di Benedetto F, Tumulero BF, Sousa DZ: **Microbial conversion of carbon dioxide and hydrogen into the fine chemicals hydroxyectoine and ectoine**. *Bioresour Technol* 2023, **374**:128753, https://doi.org/10.1016/j.biortech.2023.128753

9. Cao X, Cui L, Sun S, Li T, Wang Y, Wang S, *et al.*: **Isolation and screening of hydrogen-oxidizing bacteria from mangrove**

sediments for efficient single-cell protein production using CO_2. *Microorganisms* 2026, https://doi.org/10.3390/microorganisms14020346

10. Ishizaki A, Tanaka K: **Production of poly-β-hydroxybutyric acid from carbon dioxide by Alcaligenes eutrophus ATCC 17697T**. *J Ferment Bioeng* 1991, **71**:254-257, https://doi.org/10.1016/0922-338X(91)90277-N

11. Hogendoorn C, Pol A, Picone N, Cremers G, van Alen TA, Gagliano AL, *et al*.: **Hydrogen and carbon monoxide-utilizing *Kyrpidia spormannii* species from Pantelleria Island, Italy**. *Front Microbiol* 2020, **11**:951, https://doi.org/10.3389/fmicb.2020.00951

12. Sydow A, Krieg T, Ulber R, Holtmann D: **Growth medium and electrolyte-How to combine the different requirements on the reaction solution in bioelectrochemical systems using *Cupriavidus necator***. *Eng Life Sci* 2017, **17**:781-791, https://doi.org/10.1002/elsc.201600252

13. • Rominger L, Hackbarth M, Jung T, Scherzinger M, Rosa LFM, Horn H, *et al*.: **Efficiency and process development for microbial biomass production using oxic bioelectrosynthesis**. *Trends Biotechnol* 2025, **43**:673-695, https://doi.org/10.1016/j.tibtech.2024.11.005.

This work presents a comprehensive analysis of oMES for biomass production, including techno-economic considerations and reactor design implications.

14. Paoli GC, Tabita FR: **Aerobic chemolithoautotrophic growth and RubisCO function in *Rhodobacter capsulatus* and a spontaneous gain of function mutant of *Rhodobacter sphaeroides***. *Arch Microbiol* 1998, **170**:8-17, https://doi.org/10.1007/s002030050609

15. Siegel RS, Ollis DF: **Kinetics of growth of the hydrogen-oxidizing bacterium *Alcaligenes eutrophus* (ATCC 17707) in chemostat culture**. *Biotechnol Bioeng* 1984, **26**:764-770, https://doi.org/10.1002/bit.260260721

16. Lambauer V, Hagenbuchner C, Graber M, Wiltsche H, Subotić V, Hochenauer C, *et al*.: **Cost-efficient autotrophic high-cell-density cultivation of *Cupriavidus necator* enabled by model-based gas supply**. *Biotechnol Bioeng* 2026, **123**:92-103, https://doi.org/10.1002/bit.70079

17. Häring V, Conrad R: **Kinetics of H 2 oxidation in respiring and denitrifying *Paracoccus denitrificans***. *FEMS Microbiol Lett* 1991, **78**:259-264, https://doi.org/10.1111/j.1574-6968.1991.tb04452.x

18. Nishihara H, Igarashi Y, Kodama T: ***Hydrogenovibrio marinus* gen. nov., sp. nov., a marine obligately chemolithoautotrophic hydrogen-oxidizing bacterium**. *Int J Syst Bacteriol* 1991, **41**:130-133, https://doi.org/10.1099/00207713-41-1-130

19. Yoon K-S, Fukuda K, Fujisawa K, Nishihara H: **Purification and characterization of a highly thermostable, oxygen-resistant, respiratory [NiFe]-hydrogenase from a marine, aerobic hydrogen-oxidizing bacterium *Hydrogenovibrio marinus***. *Int J Hydrog Energy* 2011, **36**:7081-7088, https://doi.org/10.1016/j.ijhydene.2011.03.049

20. Schatz A: **Uptake of carbon dioxide, hydrogen and oxygen by *Hydrogenomonas facilis***. *J Gen Microbiol* 1952, **6**:329-335.

21. Schatz A, Bovell C: **Growth and hydrogenase activity of a new bacterium, *Hydrogenomonas facilis***. *J Bacteriol* 1952, **63**:87-98, https://doi.org/10.1128/jb.63.1.87-98.1952

22. Kim S, Jang YJ, Gong G, Lee S-M, Um Y, Kim KH, Ko JK: **Engineering *Cupriavidus necator* H16 for enhanced lithoautotrophic poly(3-hydroxybutyrate) production from CO_2**. *Microb Cell Fact* 2022, **21**:231, https://doi.org/10.1186/s12934-022-01962-7

23. Claassens NJ, Bordanaba-Florit G, Cotton CAR, Maria A de, Finger-Bou M, Friedeheim L, *et al*.: **Replacing the Calvin cycle with the reductive glycine pathway in *Cupriavidus necator***. *Metab Eng* 2020, **62**:30-41, https://doi.org/10.1016/j.ymben.2020.08.004

24. • Dronsella B, Orsi E, Schulz-Mirbach H, Benito-Vaquerizo S, Yilmaz S, Glatter T, *et al*.: **One-carbon fixation via the synthetic reductive glycine pathway exceeds yield of the Calvin cycle**. *Nat Microbiol* 2025, **10**:646-653, https://doi.org/10.1038/s41564-025-01941-9.

This work demonstrates that synthetic carbon fixation pathways can outperform the Calvin cycle in yield, highlighting the potential of engineered metabolism for efficient CO_2 conversion.

25. Taga N, Tanaka K, Ishizaki A: **Effects of rheological change by addition of carboxymethylcellulose in culture media of an air-lift fermentor on poly-D-3-hydroxybutyric acid productivity in autotrophic culture of hydrogen-oxidizing bacterium, *Alcaligenes eutrophus***. *Biotechnol Bioeng* 1997, **53**:529-533, https://doi.org/10.1002/(SICI)1097-0290(19970305)53:5<529::AID-BIT11>3.0.CO;2-B

26. Volova TG, Kalacheva GS, Altukhova OV: **The autotrophic synthesis of polyhydroxyalkanoate by *Alcaligenes eutrophus* in the presence of carbon monoxide**. *Microbiology* 2001, **70**:640, https://doi.org/10.1023/A:1013175413013

27. Volova TG, Kalacheva GS, Gorbunova OV, Zhila NO: **Dynamics of activity of the key enzymes of polyhydroxyalkanoate metabolism in *Ralstonia eutropha* B5786**. *Appl Biochem Microbiol* 2004, **40**:170-177, https://doi.org/10.1023/B:ABIM.0000018921.04863.d5

28. Volova TG, Kiselev EG, Shishatskaya EI, Zhila NO, Boyandin AN, Syrvacheva DA, *et al*.: **Cell growth and accumulation of polyhydroxyalkanoates from CO_2 and H_2 of a hydrogen-oxidizing bacterium, *Cupriavidus eutrophus* B-10646**. *Bioresour Technol* 2013, **146**:215-222, https://doi.org/10.1016/j.biortech.2013.07.070

29. Garcia-Gonzalez L, Mozumder MSI, Dubreuil M, Volcke EI, de Wever H: **Sustainable autotrophic production of polyhydroxybutyrate (PHB) from CO_2 using a two-stage cultivation system**. *Catal Today* 2015, **257**:237-245, https://doi.org/10.1016/j.cattod.2014.05.025

30. Lu Y, Yu J: **Gas mass transfer with microbial CO_2 fixation and poly(3-hydroxybutyrate) synthesis in a packed bed bioreactor**. *Biochem Eng J* 2017, **122**:13-21, https://doi.org/10.1016/j.bej.2017.02.013

31. Chen X, Cao Y, Li F, Tian Y, Song H: **Enzyme-assisted microbial electrosynthesis of poly(3-hydroxybutyrate) via CO_2 bioreduction by engineered *Ralstonia eutropha***. *ACS Catal* 2018, **8**:4429-4437, https://doi.org/10.1021/acscatal.8b00226

32. Miyahara Y, Yamamoto M, Thorbecke R, Mizuno S, Tsuge T: **Autotrophic biosynthesis of polyhydroxyalkanoate by *Ralstonia eutropha* from non-combustible gas mixture with low hydrogen content**. *Biotechnol Lett* 2020, **42**:1655-1662, https://doi.org/10.1007/s10529-020-02876-3

33. Shin SK, Ko YJ, Da Jeong W, Lee M-E, You SK, Hyeon JE, Han SO: **Enhanced production of polyhydroxybutyrate from syngas by using nanoscaled cellulose particles with a syngas-converting enzyme complex immobilized on *Ralstonia eutropha***. *J Clean Prod* 2021, **285**:124903, https://doi.org/10.1016/j.jclepro.2020.124903

34. Tanaka K, Yoshida K, Orita I, Fukui T: **Biosynthesis of poly(3-hydroxybutyrate-co-3-hydroxyhexanoate) from CO_2 by a recombinant *Cupriavidus necator***. *Bioengineering* 2021, https://doi.org/10.3390/bioengineering8110179

35. Lambauer V, Kratzer R: **Lab-scale cultivation of *Cupriavidus necator* on explosive gas mixtures: carbon dioxide fixation into polyhydroxybutyrate**. *Bioengineering* 2022, https://doi.org/10.3390/bioengineering9050204

36. Li H, Opgenorth PH, Wernick DG, Rogers S, Wu T-Y, Higashide W, *et al*.: **Integrated electromicrobial conversion of CO_2 to higher alcohols**. *Science* 2012, **335**:1596, https://doi.org/10.1126/science.1217643

37. Przybylski D, Rohwerder T, Dilßner C, Maskow T, Harms H, Müller RH: **Exploiting mixtures of H_2, CO_2, and O_2 for improved production of methacrylate precursor 2-hydroxyisobutyric acid by engineered *Cupriavidus necator* strains**. *Appl Microbiol Biotechnol* 2015, **99**:2131-2145, https://doi.org/10.1007/s00253-014-6266-6

38. Crépin L, Lombard E, Guillouet SE: **Metabolic engineering of *Cupriavidus necator* for heterotrophic and autotrophic alka(e)**

ne production. *Metab Eng* 2016, **37**:92-101, https://doi.org/10.1016/j.ymben.2016.05.002

39. Krieg T, Sydow A, Faust S, Huth I, Holtmann D: **CO_2 to terpenes: autotrophic and electroautotrophic α-humulene production with *Cupriavidus necator***. *Angew Chem Int Ed Engl* 2018, **57**:1879-1882, https://doi.org/10.1002/anie.201711302

40. Windhorst C, Gescher J: **Efficient biochemical production of acetoin from carbon dioxide using *Cupriavidus necator* H16**. *Biotechnol Biofuels* 2019, **12**:163, https://doi.org/10.1186/s13068-019-1512-x

41. • Weiler JR, Jürgensen N, Cornejo Infante M, Knoll MT, Gescher J: **Strain and model development for auto- and heterotrophic 2,3-butanediol production using *Cupriavidus necator* H16**. *Biotechnol Biofuels Bioprod* 2024, **17**:108, https://doi.org/10.1186/s13068-024-02549-7.

This work demonstrates metabolic engineering and modeling approaches enabling both autotrophic and heterotrophic production of 2,3-butanediol in *C. necator*.

42. Garrigues L, Maignien L, Lombard E, Singh J, Guillouet SE: **Isopropanol production from carbon dioxide in *Cupriavidus necator* in a pressurized bioreactor**. *N Biotechnol* 2020, **56**:16-20, https://doi.org/10.1016/j.nbt.2019.11.005

43. • Ma C, Cheng X, Wang Y, Chen K, Ma Y, Lin Y, *et al.*: **High-efficiency CO_2 fixation and single-cell protein production in *Cupriavidus necator* via ARTP-driven metabolic rewiring**. *Green Chem* 2026, **28**:4550-4563, https://doi.org/10.1039/D5GC05791D.

This work presents improved CO_2 fixation and single-cell protein production in *C. necator* through ARTP-driven metabolic rewiring, highlighting the potential of strain engineering to enhance autotrophic biomass productivity.

44. Mandel C, Edel M, Gescher J: **Opinion on biofilms as production systems**. *Microb Biotechnol* 2025, **18**:e70182, https://doi.org/10.1111/1751-7915.70182

45. Diankristanti PA, Lin Y-C, Yi Y-C, Ng I-S: **Polyhydroxyalkanoates bioproduction from bench to industry: thirty years of development towards sustainability**. *Bioresour Technol* 2024, **393**:130149, https://doi.org/10.1016/j.biortech.2023.130149

46. Schlegel HG, Gottschalk G, von Bartha R: **Formation and utilization of poly-beta-hydroxybutyric acid by Knallgas bacteria (*Hydrogenomonas*)**. *Nature* 1961, **191**:463-465, https://doi.org/10.1038/191463a0

47. Ishizaki A, Tanaka K, Taga N: **Microbial production of poly-D-3-hydroxybutyrate from CO_2**. *Appl Microbiol Biotechnol* 2001, **57**:6-12, https://doi.org/10.1007/s002530100775

48. Kracke F, Deutzmann JS, Jayathilake BS, Pang SH, Chandrasekaran S, Baker SE, Spormann AM: **Efficient hydrogen delivery for microbial electrosynthesis via 3D-printed cathodes**. *Front Microbiol* 2021, **12**:696473, https://doi.org/10.3389/fmicb.2021.696473

49. Popat SC, Torres CI: **Critical transport rates that limit the performance of microbial electrochemistry technologies**. *Bioresour Technol* 2016, **215**:265-273, https://doi.org/10.1016/j.biortech.2016.04.136

50. Coward HF, Jones GW: **Limits of flammability of gases and vapors**. *Bulletin 503, U.S. Bureau of Mines, Washington, D.C._ *1952*; 1952.

51. Lewis B, von Elbe G: **Combustion, Flames, and Explosions of Gases**. 3rd edn, Academic Press; 1987.

52. Zlochower IA, Green GM: **The limiting oxygen concentration and flammability limits of gases and gas mixtures**. *J Loss Prev Process Ind* 2009, **22**:499-505, https://doi.org/10.1016/j.jlp.2009.03.006

53. Gross R, Lang K, Bühler K, Schmid A: **Characterization of a biofilm membrane reactor and its prospects for fine chemical synthesis**. *Biotechnol Bioeng* 2010, **105**:705-717, https://doi.org/10.1002/bit.22584

54. Gross R, Buehler K, Schmid A: **Engineered catalytic biofilms for continuous large scale production of n-octanol and (S)-styrene oxide**. *Biotechnol Bioeng* 2013, **110**:424-436, https://doi.org/10.1002/bit.24629

55. Renaudie M, Dumas C, Vuilleumier S, Ernst B: **Biohydrogen production in a continuous liquid/gas hollow fiber membrane bioreactor: efficient retention of hydrogen producing bacteria via granule and biofilm formation**. *Bioresour Technol* 2021, **319**:124203, https://doi.org/10.1016/j.biortech.2020.124203

56. Jourdin L, Freguia S, Donose BC, Chen J, Wallace GG, Keller J, Flexer V: **A novel carbon nanotube modified scaffold as an efficient biocathode material for improved microbial electrosynthesis**. *J Mater Chem A* 2014, **2**:13093-13102, https://doi.org/10.1039/c4ta03101f

57. Krieg T, Sydow A, Schröder U, Schrader J, Holtmann D: **Reactor concepts for bioelectrochemical syntheses and energy conversion**. *Trends Biotechnol* 2014, **32**:645-655, https://doi.org/10.1016/j.tibtech.2014.10.004

58. • Cabau-Peinado O, Winkelhorst M, Stroek R, de Kat Angelino R, Straathof AJJ, Masania K, *et al.*: **Microbial electrosynthesis from CO_2 reaches productivity of syngas and chain elongation fermentations**. *Trends Biotechnol* 2024, **42**:1503-1522, https://doi.org/10.1016/j.tibtech.2024.06.005.

This work presents that microbial electrosynthesis can achieve volumetric productivities comparable to established fermentation processes, challenging the perception that bioelectrochemical systems are inherently rate-limited.

59. Weiler J, Edel M, Gescher J: **Biofilms for production of chemicals and energy**. *Annu Rev Chem Biomol Eng* 2024, **15**:361-387, https://doi.org/10.1146/annurev-chembioeng-100522-110939